Broadband X-ray Study of the Galactic Microquasar W50/SS433, a Galactic PeVatron Candidate

Brydyn Mac Intyre

TeVPA 2022
August 10

University of Manitoba
macintyb@myumanitoba.ca

TRADITIONAL TERRITORIES ACKNOWLEDGEMENT

The University of Manitoba campuses are located on original lands of Anishinaabeg, Cree, Oji-Cree, Dakota, and Dene peoples, and on the homeland of the Métis Nation.

We respect the Treaties that were made on these territories, we acknowledge the harms and mistakes of the past, and we dedicate ourselves to move forward in partnership with Indigenous communities in a spirit of reconciliation and collaboration.

Acknowledgement of Territory

Queen's University is situated on traditional Anishinaabe and Haudenosaunee Territory. To acknowledge this traditional territory is to recognize its longer history, one predating the establishment of the earliest European colonies. It is also to acknowledge this territory's significance for the Indigenous peoples who lived, and continue to live, upon it – people whose practices and spiritualities were tied to the land and continue to develop in relationship to the territory and its other inhabitants today.

The Kingston Indigenous community continues to reflect the area's Anishinaabek and Haudenosaunee roots. There is also a significant Métis community and there are First Peoples from other Nations across Turtle Island present here today.

The team (W50-east)

Univ.of Manitoba

SSH

Brydyn Mac Intyre

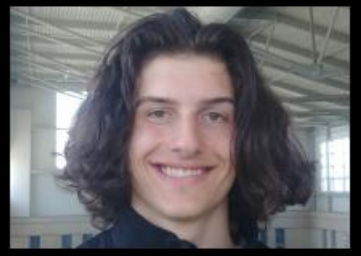

Matthew Band

Chelsea Braun

Shuo Zhang
(Bard College)

Columbia Univ.

Kaya Mori

Isaac Pope

Shuhan Zhang

Nate Saffold

Chuck Hailey

Eric Gotthelf

Felix Aharonian
(DIAS/MPIK)

Mel Nynka (MIT)

Ke Fang (U.Wisconsin)

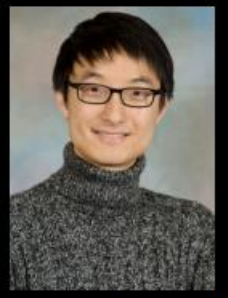

Chang D Rho (Seoul)

Cosmic Rays

Cosmic rays hitting Earth.
Credit: (NSF/J. Yang)

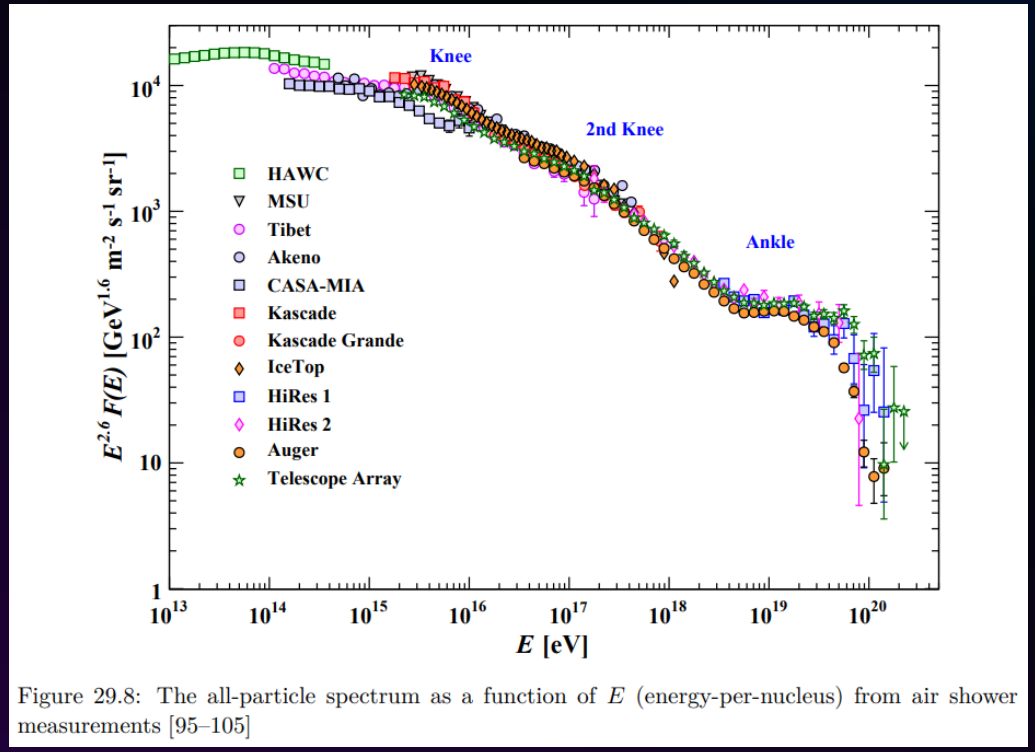

Figure 29.8: The all-particle spectrum as a function of E (energy-per-nucleus) from air shower measurements [95–105]

https://pdg.lbl.gov/2019/reviews/rpp2019-rev-cosmic-rays.pdf

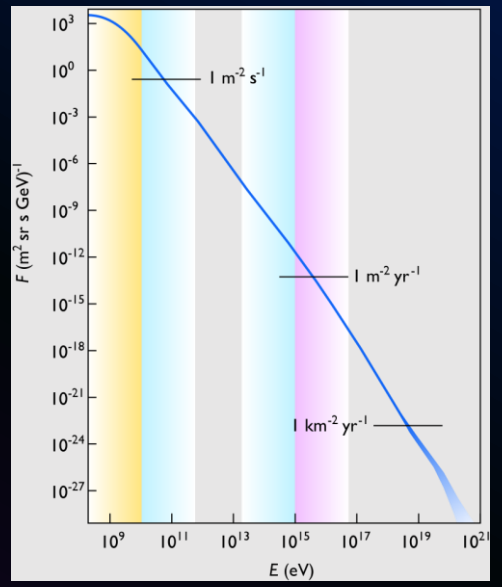

By Sven Lafebre, after Swordy and De Angelis, CC BY-SA 3.0

Background – Supernova Remnants (SNRs)

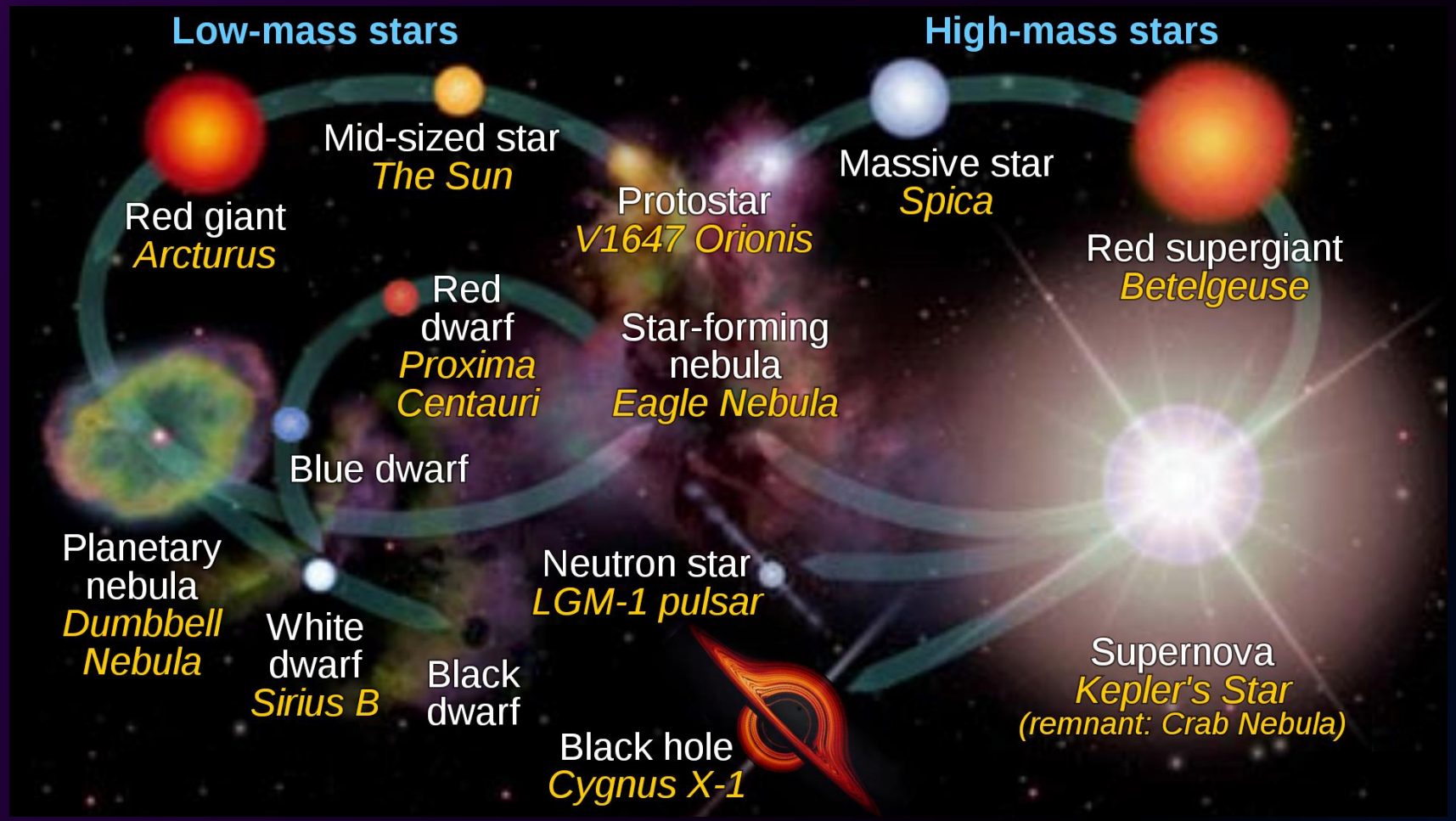

By cmglee, NASA Goddard Space Flight Center, CC BY-SA 4.0

Background - Microquasars

Quasar

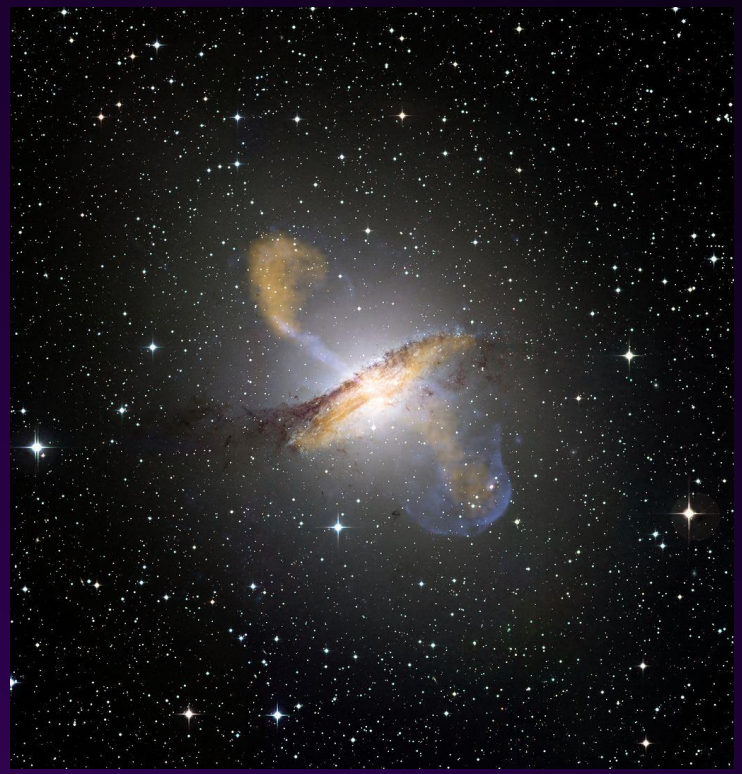

By ESO/WFI, CC BY 4.0

Microquasar

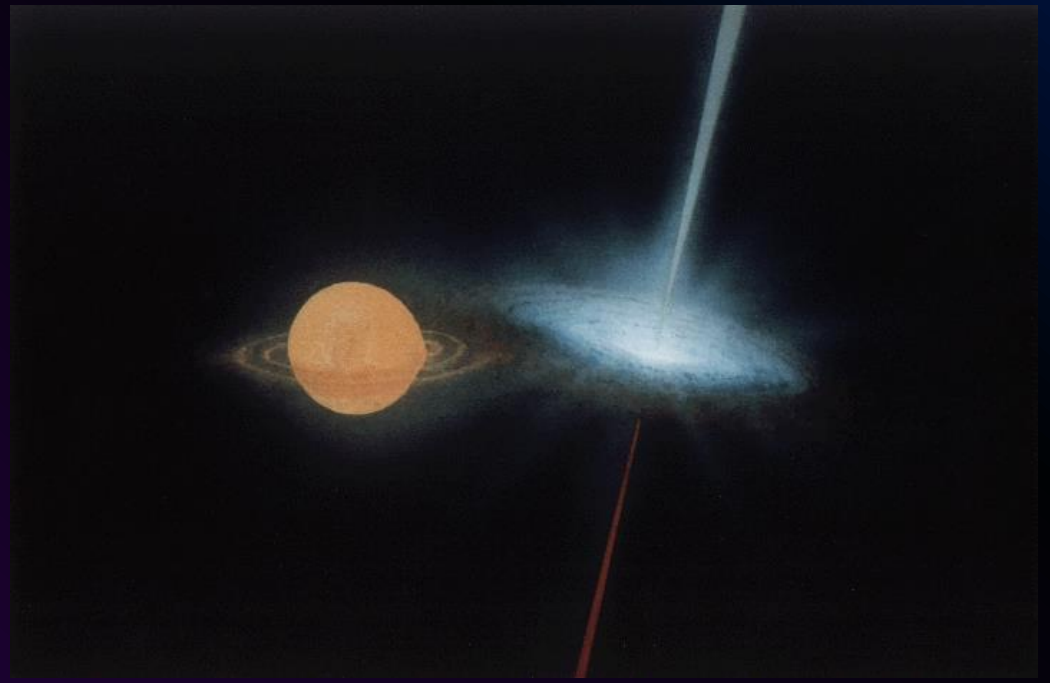

By NASA - https://apod.nasa.gov/apod/ap960306.html

SS 433 and W50

Credit: DESY, Science Communication Lab

HAWC 2018

- Detected TeV emission from W50
- 20 year old predictions confirmed

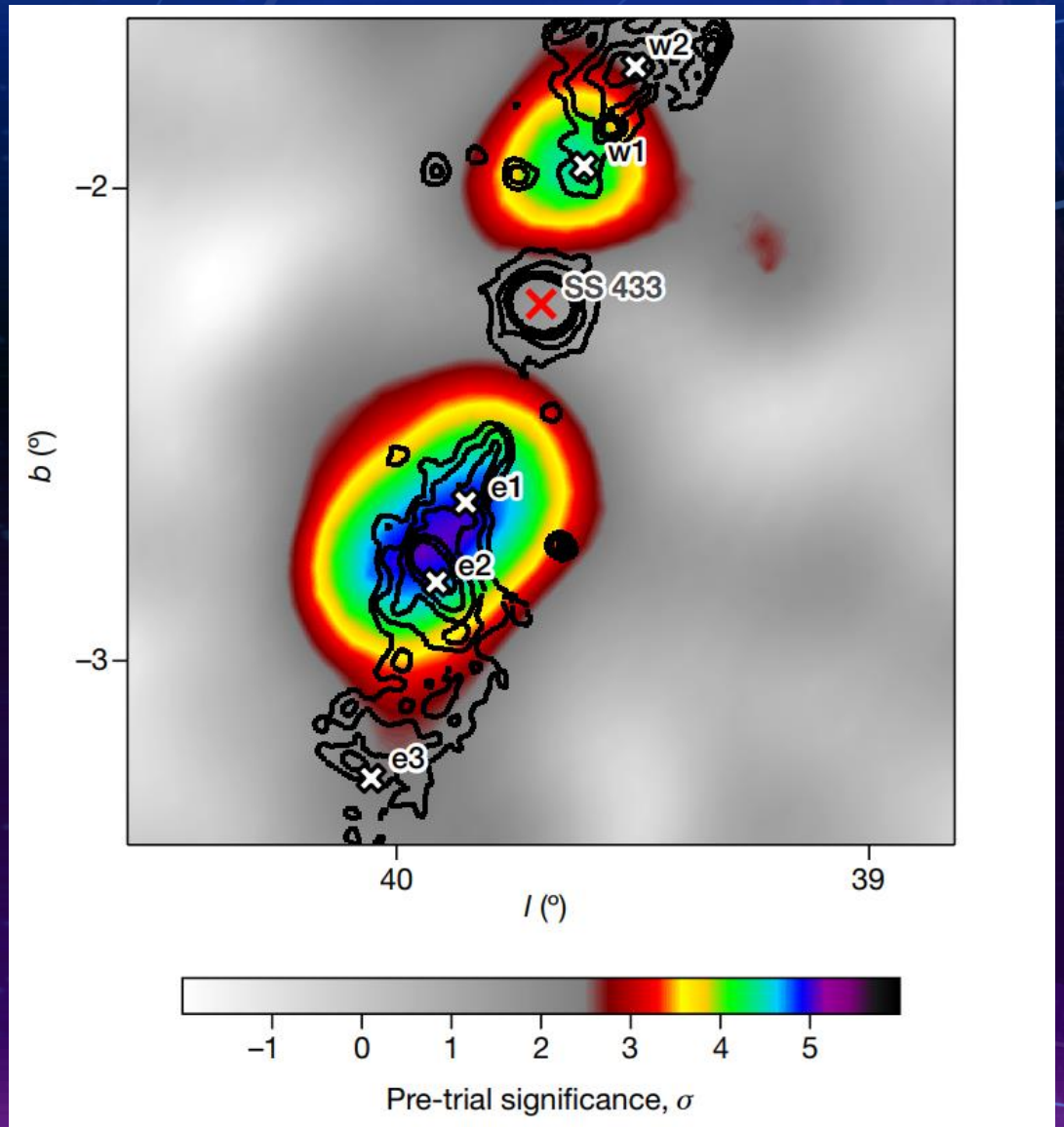

Abeysekara, A.U., Albert, A., Alfaro, R. et al. Very-high-energy particle acceleration powered by the jets of the microquasar SS 433. Nature 562, 82–85 (2018). https://doi.org/10.1038/s41586-018-0565-5

This Research

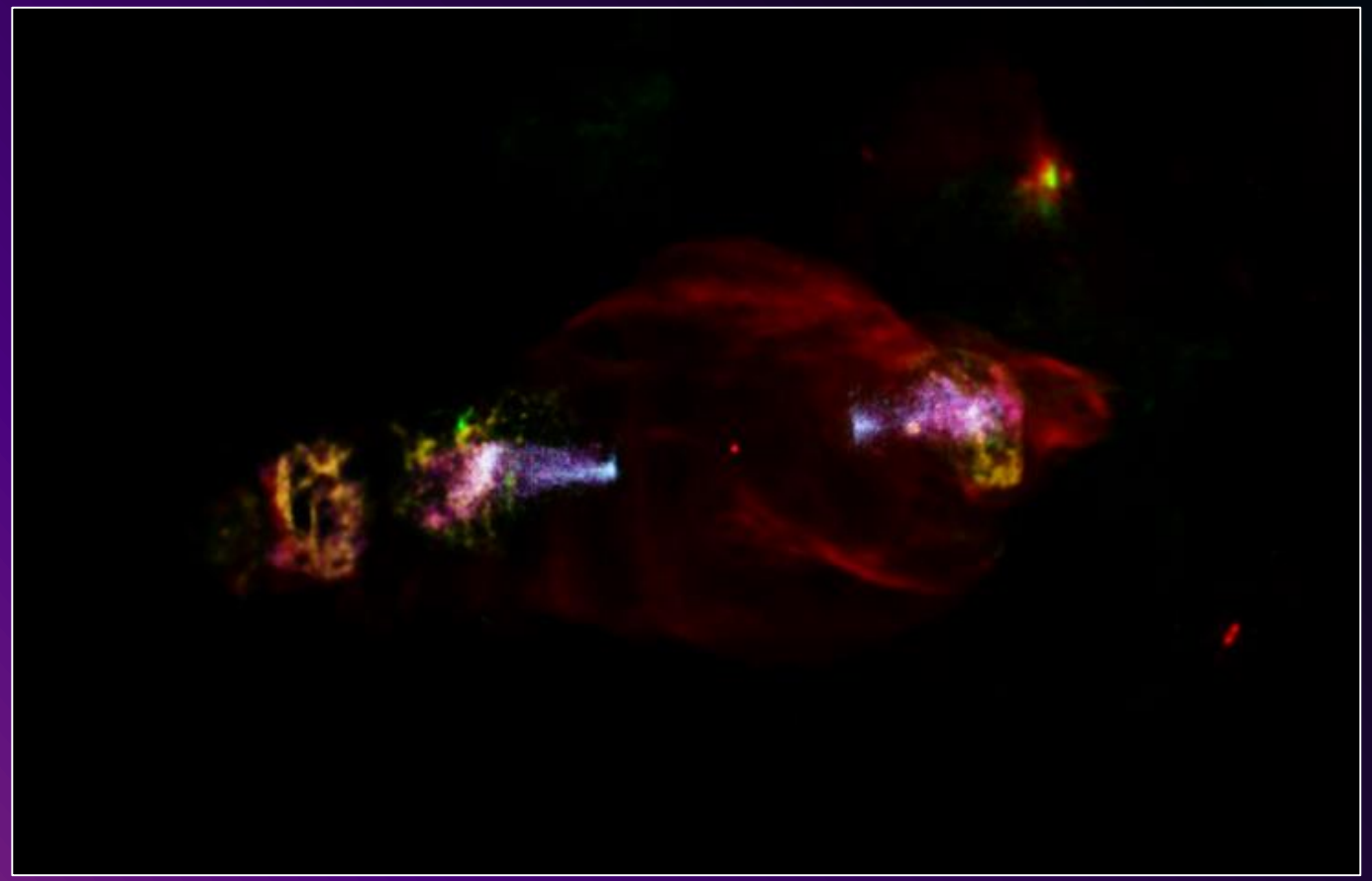

Hard X-ray emission from the eastern jet of SS 433 powering the W50 'Manatee' nebula: Evidence for particle re-acceleration

S. Safi-Harb,[1] B. Mac Intyre,[1] S. Zhang,[2] I. Pope,[3] S. Zhang,[3] N. Saffold,[4] K. Mori,[3] E. V. Gotthelf,[3] F. Aharonian,[5,6] M. Band,[1] C. Braun,[1] K. Fang,[7] C. Hailey,[3] M. Nynka,[8] and C. D. Rho[9]

[1] *University of Manitoba, Department of Physics & Astronomy, Winnipeg, MB R3T 2N2, Canada*
[2] *Bard College Physics Program, 30 Campus Road, Annandale-On-Hudson, NY 12504, USA*
[3] *Columbia Astrophysics Laboratory, 550 West 120th Street, New York, NY 10027, USA*
[4] *Fermi National Accelerator Laboratory, PO Box 500, Batavia IL, 60510, USA*
[5] *Dublin Institute for Advanced Studies, 31 Fitzwilliam Place, Dublin, Ireland*
[6] *Max-Planck-Institut for Nuclear Physics, P.O. Box 103980, 69029 Heidelberg, Germany*
[7] *Department of Physics, Wisconsin IceCube Particle Astrophysics Center, University of Wisconsin, Madison, WI, 53706, USA*
[8] *Kavli Institute For Astrophysics and Space Research, Massachusetts Institute of Technology, Cambridge, MA, USA*
[9] *University of Seoul, Seoul, Rep. of Korea*

ABSTRACT

We present a broadband X-ray study of W50 ('the Manatee nebula'), the complex region powered by the microquasar SS 433, that provides a test-bed for several important astrophysical processes. The W50 nebula, a Galactic PeVatron candidate, is classified as a supernova remnant but has an unusual double-lobed morphology likely associated with the jets from SS 433. Using NuSTAR, XMM-Newton, and Chandra observations of the inner eastern lobe of W50, we have detected hard non-thermal X-ray emission up to ∼30 keV, originating from a few-arcminute size knotty region ('Head') located $\lesssim 18'$ (29 pc for a distance of 5.5 kpc) east of SS 433, and constrain its photon index to 1.58±0.05 (0.5–30 keV band). The index gradually steepens eastward out to the radio 'ear' where thermal soft X-ray emission with a temperature kT∼0.2 keV dominates. The hard X-ray knots mark the location of acceleration sites within the jet and require an equipartition magnetic field of the order of $\gtrsim 12\mu$G. The unusually hard spectral index from the 'Head' region challenges classical particle acceleration processes and points to particle injection and re-acceleration in the sub-relativistic SS 433 jet, as seen in blazars and pulsar wind nebulae.

Red: Radio (Dubner et al. 1998)
Green: Optical (Boumis et al. 2007)
Yellow: 0.5-1.0 keV
Magenta : 1.0-2.0 keV
Cyan: 2.0-12.0 keV

Contents

History – Radio/Optical

- ~50 years of study!
- Optical > Radio > X-Ray
- Clark & Murdin (1978)
- Doppler Shifts
- Jets, jets, and jets

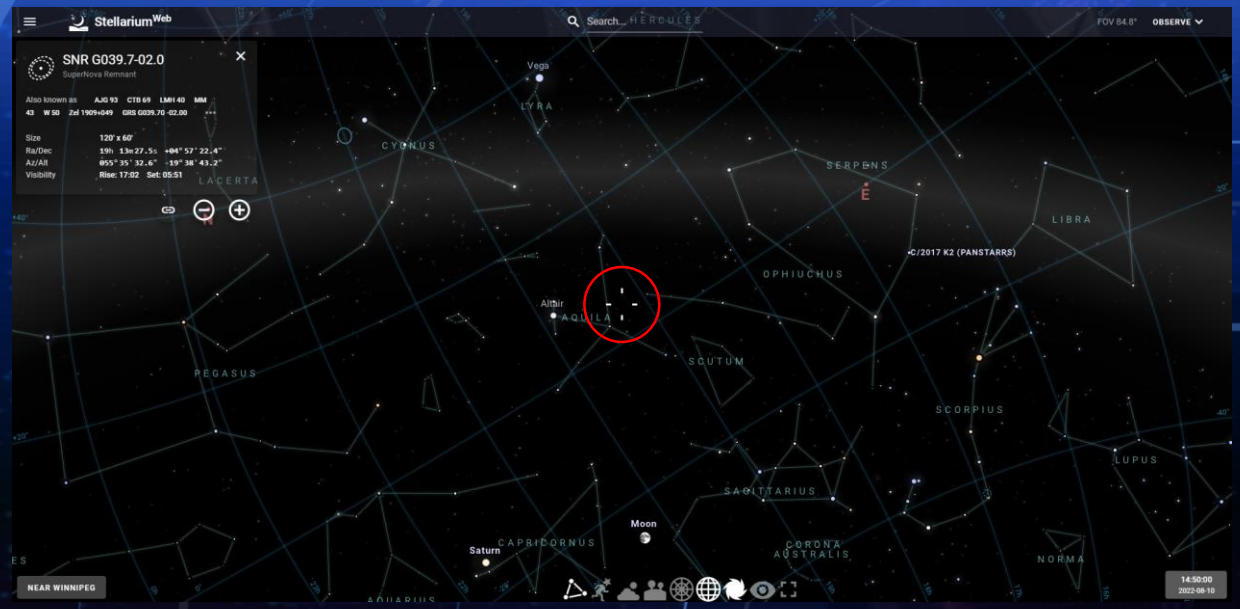

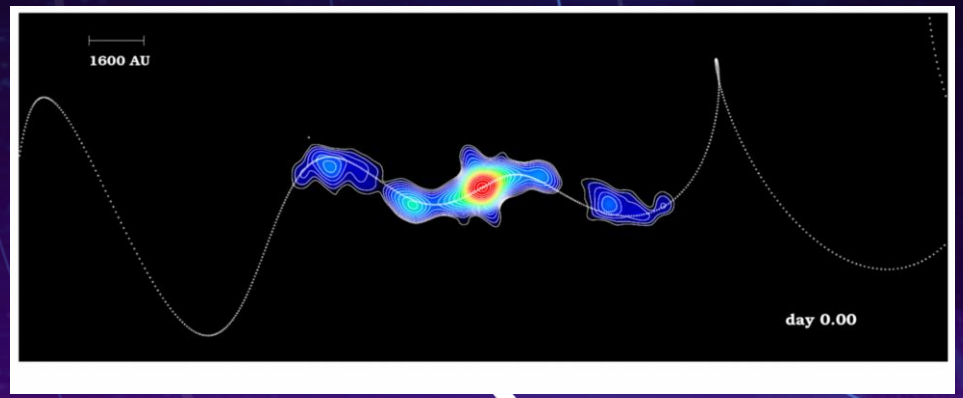

Observed precession of SS433 jets
CREDIT: A. Mioduszewski et al., NRAO/AUI/NSF

History – X-Rays (+)

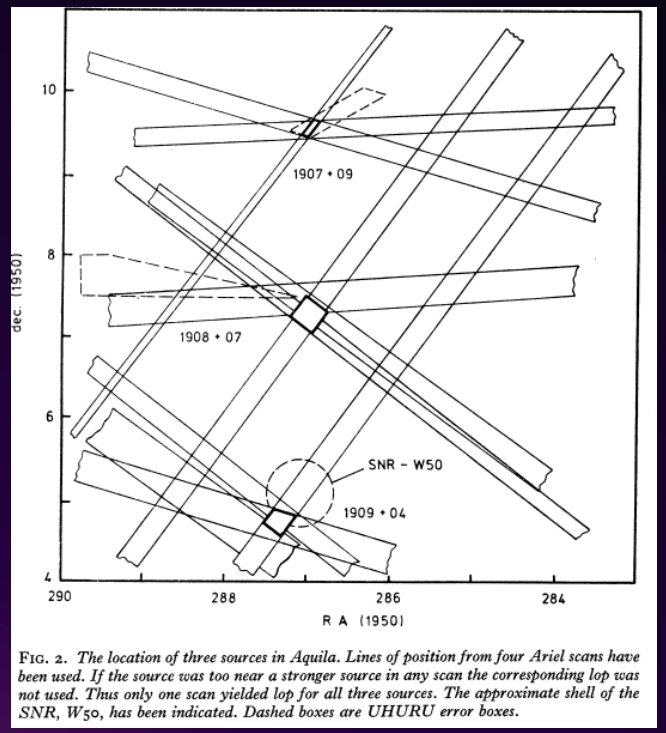

FIG. 2. *The location of three sources in Aquila. Lines of position from four Ariel scans have been used. If the source was too near a stronger source in any scan the corresponding lop was not used. Thus only one scan yielded lop for all three sources. The approximate shell of the SNR, W50, has been indicated. Dashed boxes are UHURU error boxes.*

F. D. Seward, 1976, MNRAS

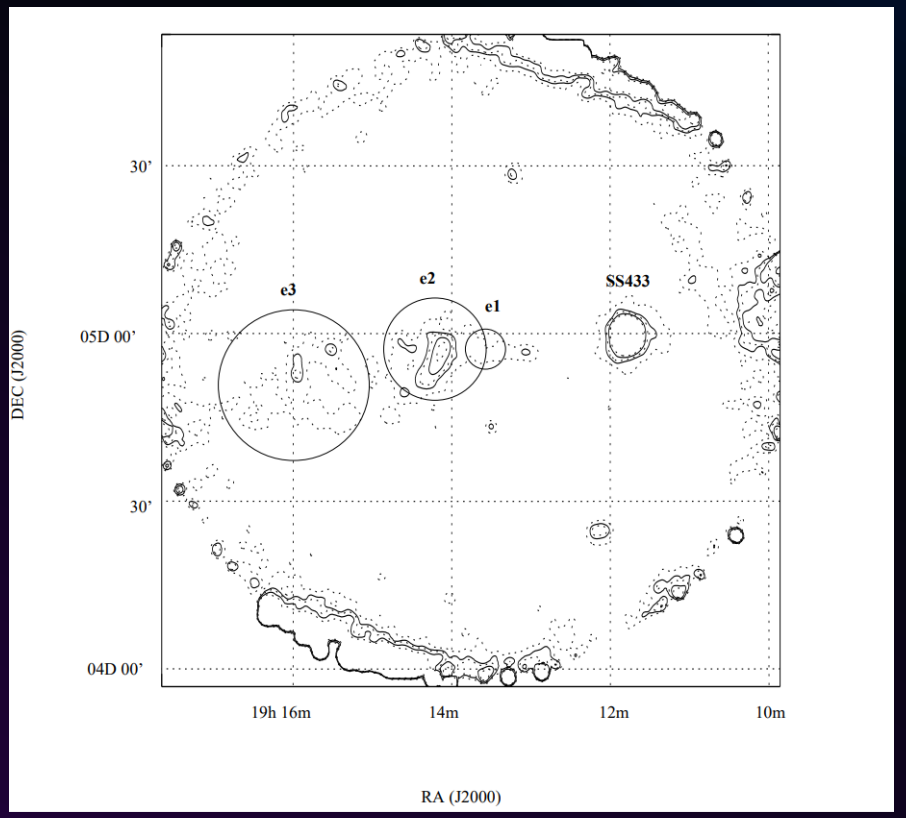

Samar Safi-Harb and Hakki Ögelman, 1997, *ApJ*

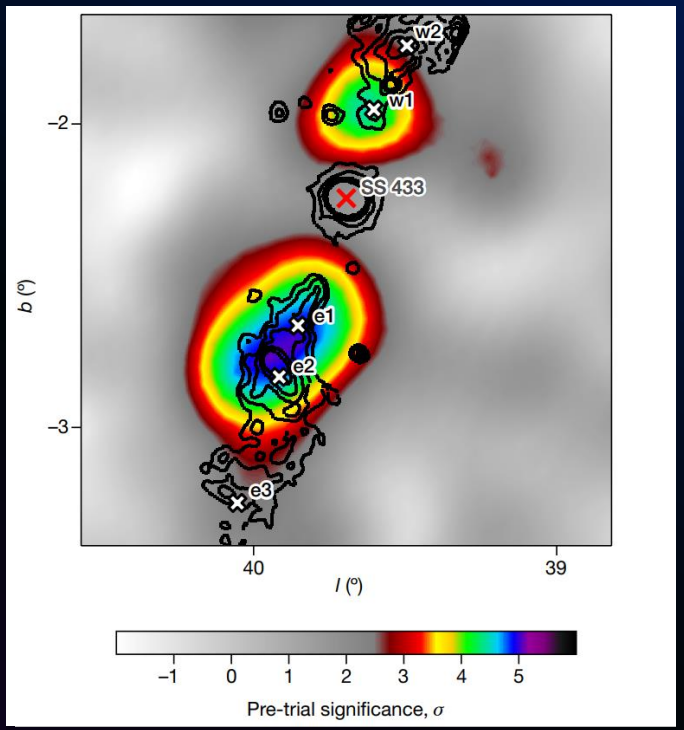

Abeysekara, A.U., et al., 2018, Nature

The Data

Chandra

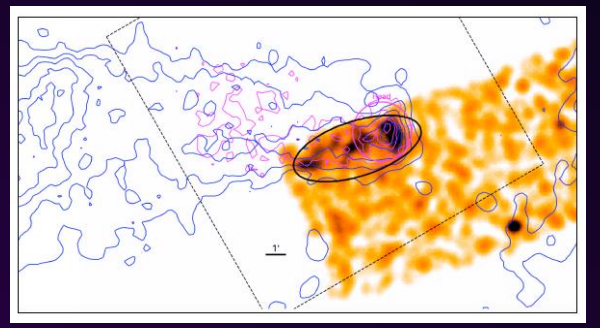

XMM-Newton

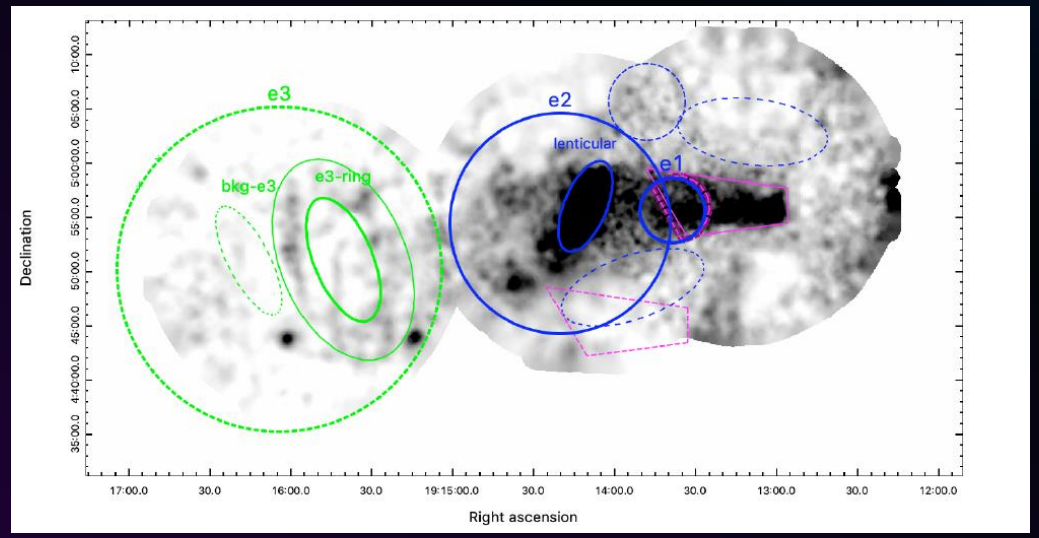

NuSTAR

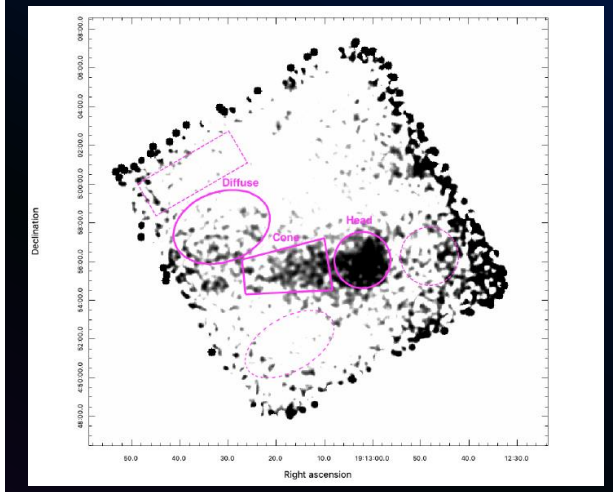

Telescopes

Chandra

- July 23, 1999
- F.o.V.: 30 arcmin
- Range: 0.1-10 keV
- Resolution: 0.5 arcsec

XMM-Newton

- December 10, 1999
- F.o.V.: 30 arcmin
- Range: 0.15-12 keV
- Resolution: 5-14 arcsec

NuSTAR

- June 13, 2012
- F.o.V.: 12 arcmin
- Range: 3-79 keV
- Resolution: 9.5 arcsec

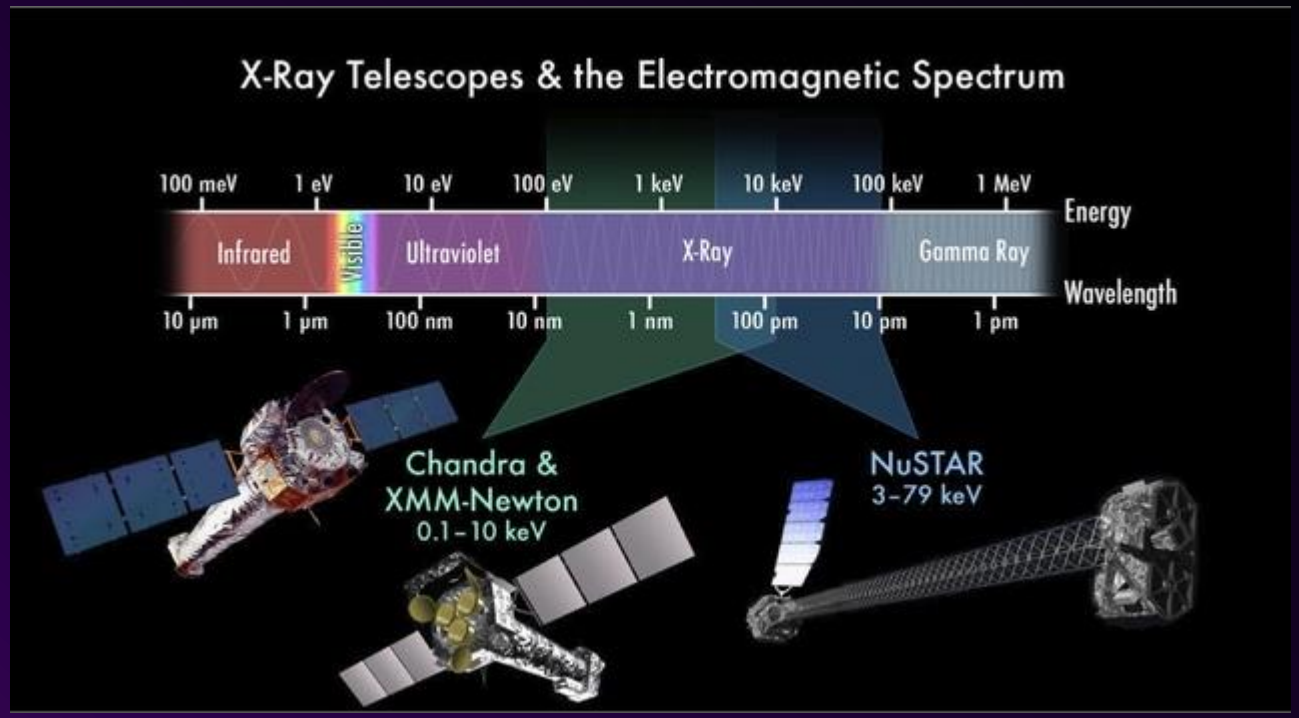

https://www.nustar.caltech.edu/page/about

Imaging Analysis

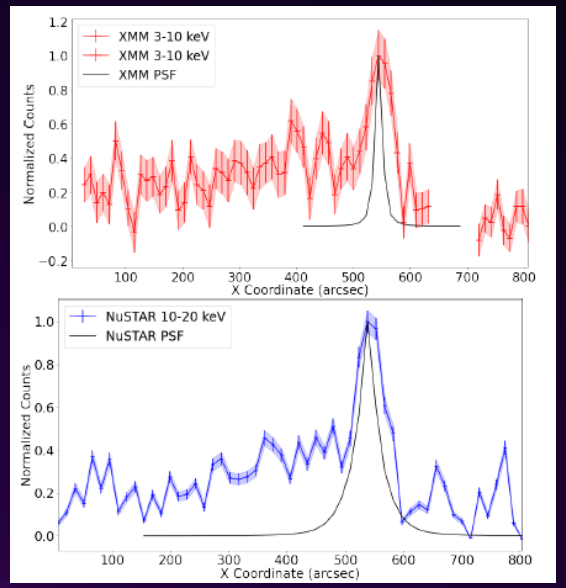

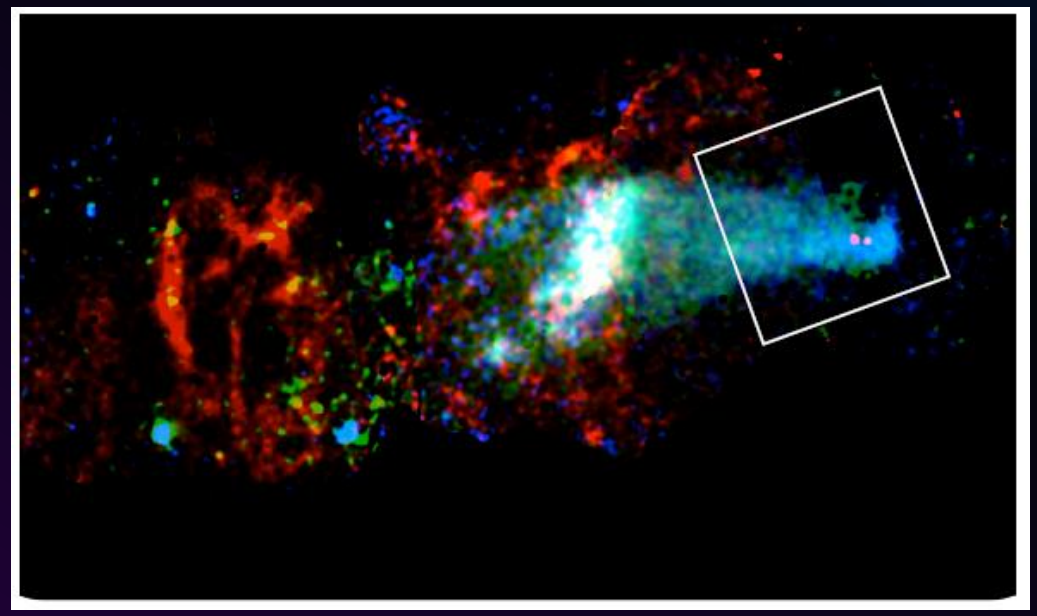

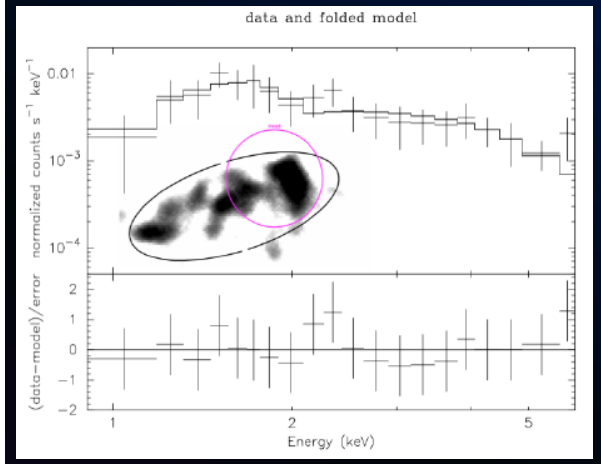

Spectral Analysis

- Exhaustive background analysis
- NuSTAR – XMM Coordination
- nH values from XMM

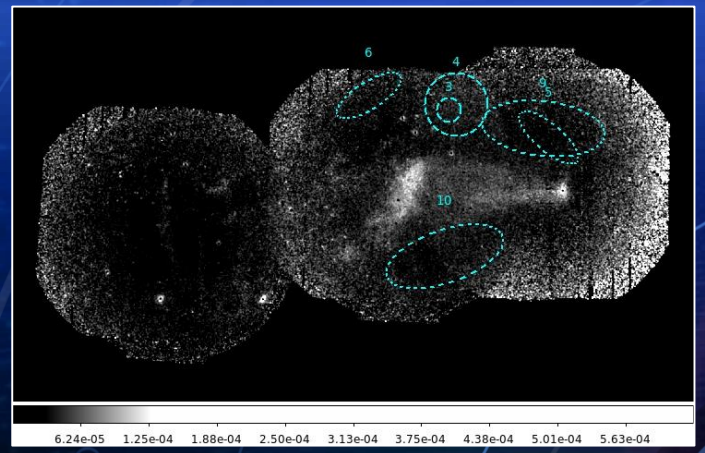

XMM

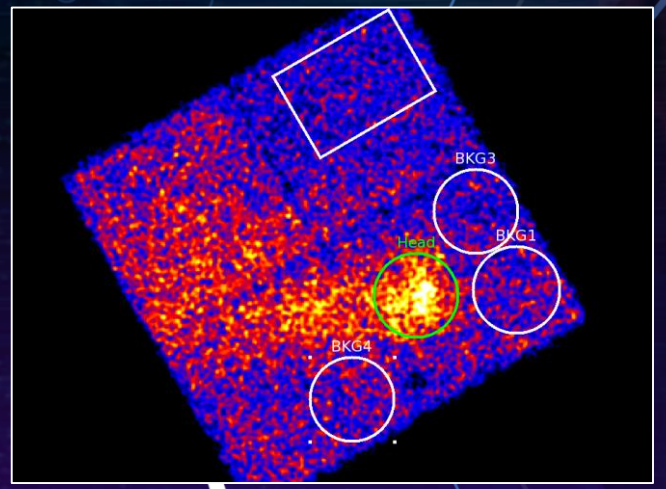

NuSTAR

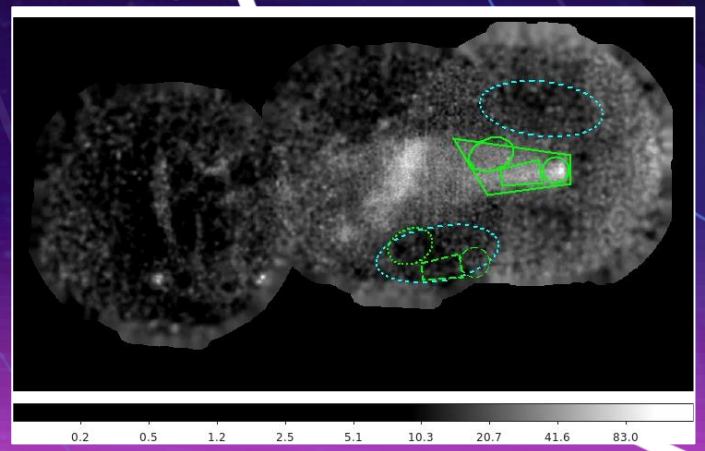

XMM

Spectral Analysis

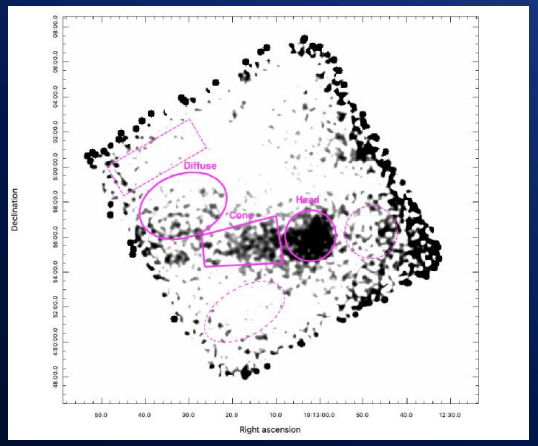

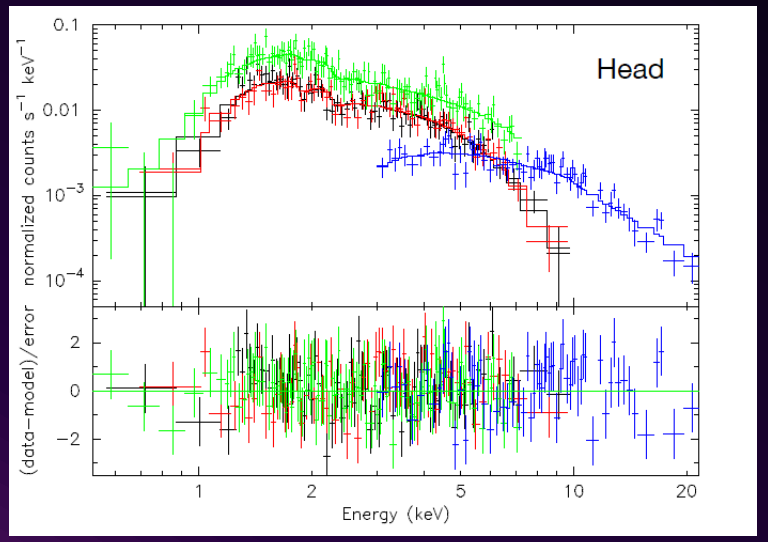

nH: 1.77x10^{22} cm^{-2}
γ: 1.58

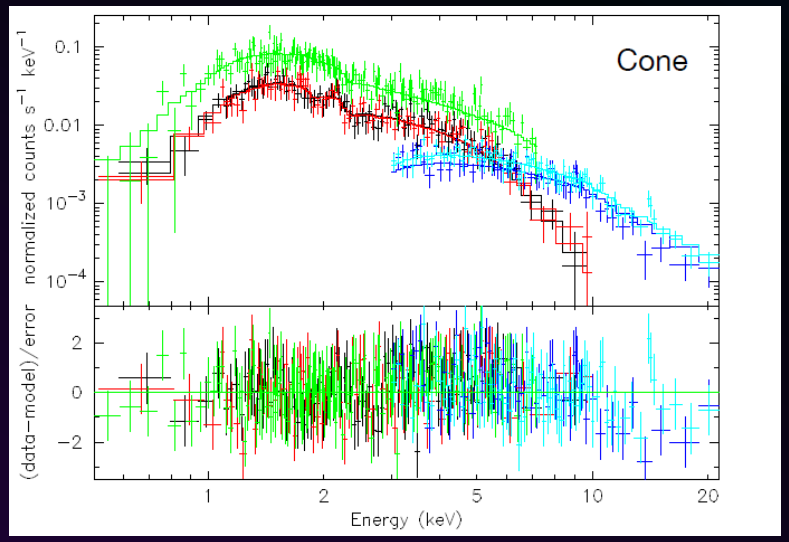

nH: 1. 18x10^{22} cm^{-2}
γ: 1.76

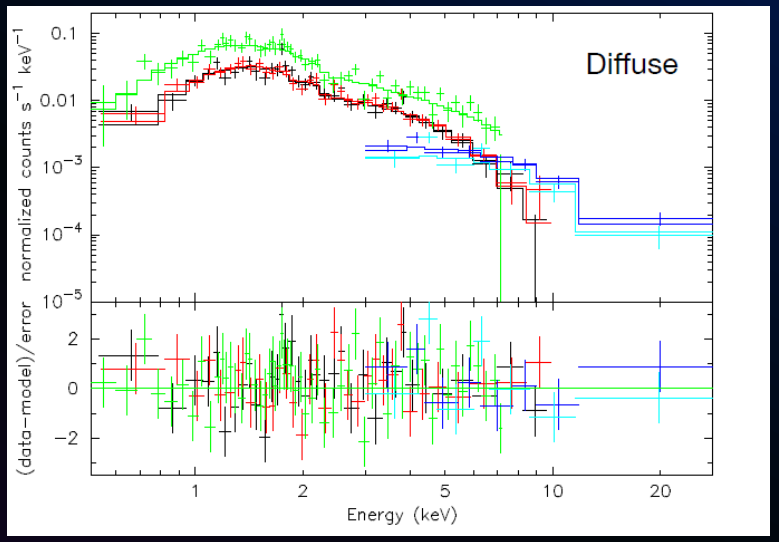

nH: 0.76x10^{22} cm^{-2}
γ: 1.77

Discussion & Conclusions

- Head represents an acceleration zone
- Radio: FRII / X-rays: FRI
- *Synchrotron*/Compton/Thermal
- Hard spectral index
  - Par. Ind. ~2, E.D. α $1/E^2$
- AGN knots
  - Pho. Ind. ~1.1-1.6
- Efficient particle acceleration!
  - 12 μG
  - ~250 TeV

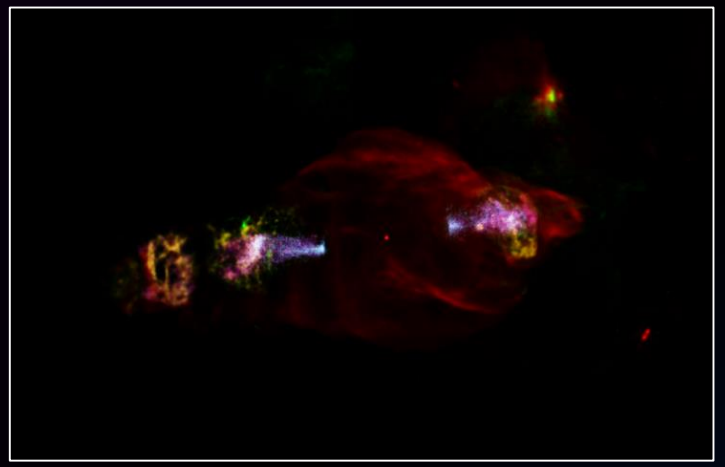

	Parameter	XMM 0.5 – 10 keV	NuSTAR 3 – 30 keV	Joint 0.5 – 30 keV[c]
Head	Photon Index Γ	1.58 ± 0.06	1.6 ± 0.1	1.58 ± 0.05
$N_H = 1.77 \times 10^{22}$ cm^{-2}	$F\,[\times 10^{-12}]^{a,c}$ (abs.)	1.23 ± 0.06	2.0 ± 0.1	2.45 ± 0.07
	$F\,[\times 10^{-12}]^{b,c}$ (unabs.)	1.80 ± 0.06	2.0 ± 0.1	3.0 ± 0.1
	χ^2_ν (DoF)	0.96(295)	1.19(79)	1.00 (375)

Future Work

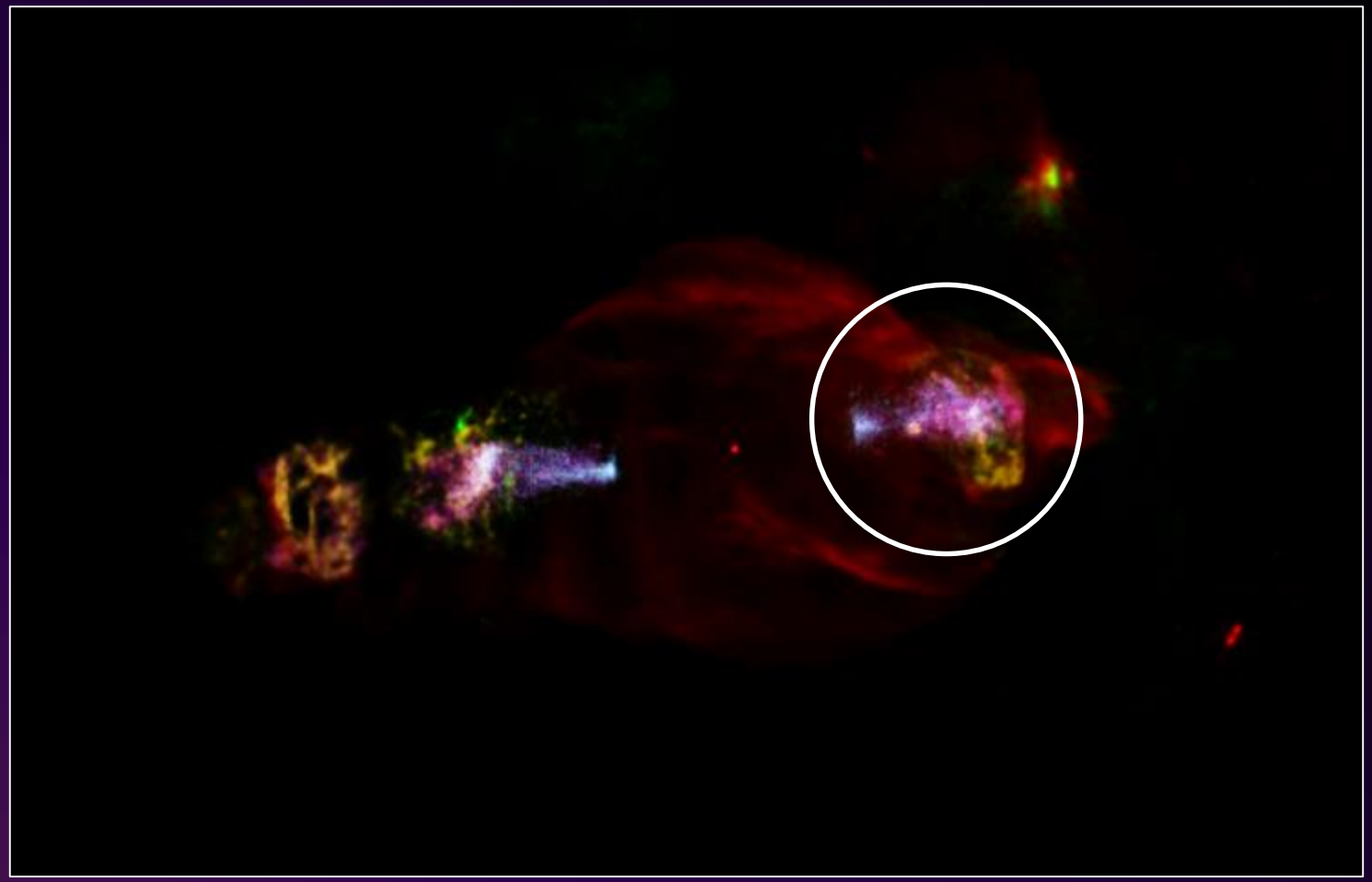

~30 arcsec

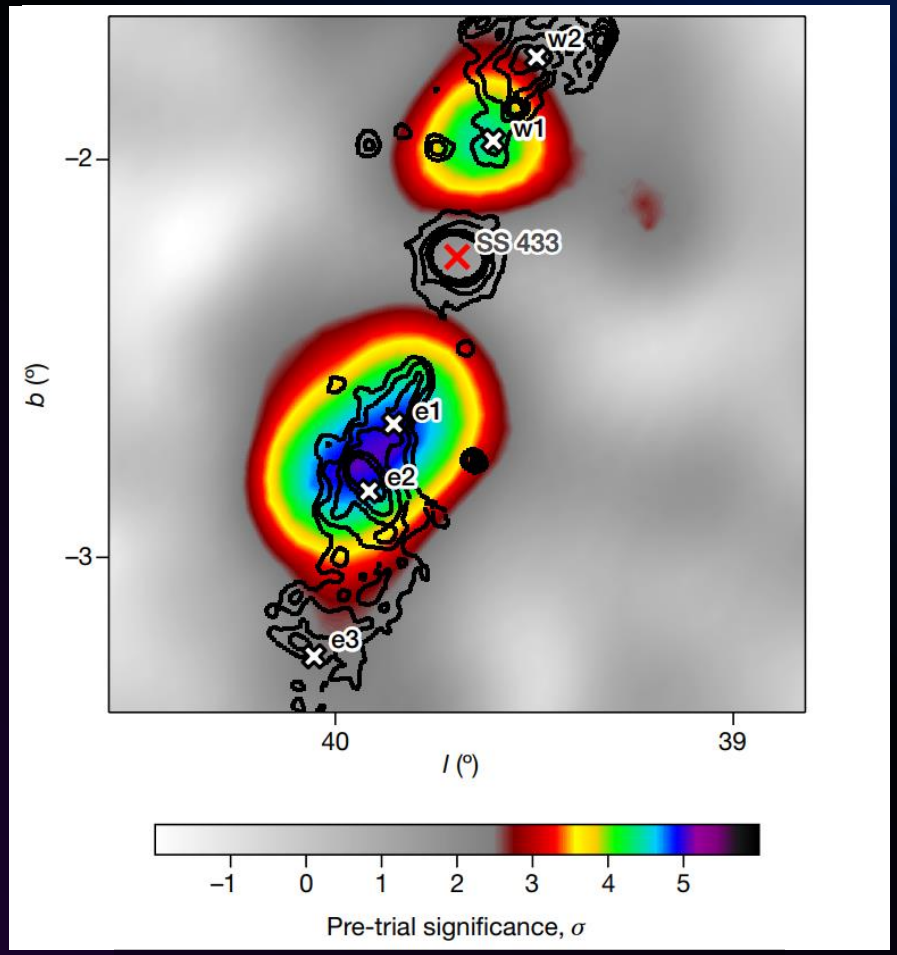

Abeysekara, A.U., et al., 2018, Nature

Thank you!

Brydyn Mac Intyre

macintyb@myumanitoba.ca

Special thanks to the W50 Collaboration!

Questions?

References

- By Sven Lafebre - own work, after Swordy(1) and De Angelis(2), CC BY-SA 3.0, https://commons.wikimedia.org/w/index.php?curid=1555202
- By cmglee, NASA Goddard Space Flight Center - Star life cycles red dwarf.jpgBlack hole's accretion disk blank.jpg, CC BY-SA 4.0, https://commons.wikimedia.org/w/index.php?curid=39174476
- By NASA - https://apod.nasa.gov/apod/ap960306.html, Public Domain, https://commons.wikimedia.org/w/index.php?curid=2978752
- By ESO/WFI (Optical); MPIfR/ESO/APEX/A.Weiss et al. (Submillimetre); NASA/CXC/CfA/R.Kraft et al. (X-ray) - http://www.eso.org/public/images/eso0903a/, CC BY 4.0, https://commons.wikimedia.org/w/index.php?curid=5821706
- F. D. Seward, C. G. Page, M. J. L. Turner, K. A. Pounds, X-ray Sources in the Aquila–Serpens–Scutum Region, *Monthly Notices of the Royal Astronomical Society*, Volume 175, Issue 1, April 1976, Pages 39P–46P, https://doi.org/10.1093/mnras/175.1.39P
- Abeysekara, A.U., Albert, A., Alfaro, R. et al. Very-high-energy particle acceleration powered by the jets of the microquasar SS 433. Nature 562, 82–85 (2018). https://doi.org/10.1038/s41586-018-0565-5
- Samar Safi-Harb and Hakki Ögelman 1997 *ApJ* **483** 868

	Parameter	XMM 0.5 – 10 keV	NuSTAR 3 – 30 keV	Joint 0.5 – 30 keV[c]
	Photon Index Γ	1.58 ± 0.06	1.6 ± 0.1	1.58 ± 0.05
Head	$F\left[\times 10^{-12}\right]^{a,c}$ (abs.)	1.23 ± 0.06	2.0 ± 0.1	2.45 ± 0.07
$N_{\rm H} = 1.77 \times 10^{22}$ cm^{-2}	$F\left[\times 10^{-12}\right]^{b,c}$ (unabs.)	1.80 ± 0.06	2.0 ± 0.1	3.0 ± 0.1
	χ^2_ν (DoF)	0.96(295)	1.19(79)	1.00 (375)
	Photon Index Γ	1.65 ± 0.05	$2.00^{+0.08}_{-0.07}$	1.76 ± 0.04
Cone	$F\left[\times 10^{-12}\right]^{a}$ (abs.)	1.29 ± 0.05	1.55 ± 0.09	2.13 ± 0.06
$N_{\rm H} = 1.18 \times 10^{22}$ cm^{-2}	$F\left[\times 10^{-12}\right]^{b}$ (unabs.)	1.81 ± 0.06	$1.58^{+0.10}_{-0.09}$	2.71 ± 0.08
	χ^2_ν (DoF)	0.96 (440)	0.98 (197)	1.03 (638)
	Photon Index Γ	1.75 ± 0.06	2.0 ± 0.2	1.77 ± 0.06
Diffuse	$F\left[\times 10^{-12}\right]^{a}$ (abs.)	$1.02^{+0.06}_{-0.05}$	$1.00^{+0.05}_{-0.14}$	1.61 ± 0.08
$N_{\rm H} = 0.76 \times 10^{22}$ cm^{-2}	$F\left[\times 10^{-12}\right]^{b}$ (unabs.)	1.39 ± 0.06	$1.00^{+0.15}_{-0.14}$	1.99 ± 0.09
	χ^2_ν (DoF)	0.98 (467)	1.33 (59)	1.02 (527)
	Photon Index Γ	1.58 ± 0.03	1.99 ± 0.07	1.65 ± 0.03
Full	$F\left[\times 10^{-12}\right]^{a}$ (abs.)	5.60 ± 0.14	8.8 ± 0.4	11.4 ± 0.2
$N_{\rm H} = 1.03 \times 10^{22}$ cm^{-2}	$F\left[\times 10^{-12}\right]^{b}$ (unabs.)	7.5 ± 0.2	9.0 ± 0.4	13.4 ± 0.2
	χ^2_ν (DoF)	1.03 (1589)	0.97 (98)	1.07 (1688)
	Photon Index Γ	1.73 ± 0.05	2.2 ± 0.2	1.76 ± 0.05
Nue1	$F\left[\times 10^{-12}\right]^{a}$ (abs.)	1.62 ± 0.07	2.0 ± 0.2	2.89 ± 0.19
$N_{\rm H} = 0.78 \times 10^{22}$ cm^{-2}	$F\left[\times 10^{-12}\right]^{b}$ (unabs.)	2.20 ± 0.08	2.0 ± 0.2	3.48 ± 0.12
	χ^2_ν (DoF)	1.05 (652)	1.53 (35)	1.09 (688)
	Photon Index Γ	2.05 ± 0.02	–	–
Lenticular[d]	$F\left[\times 10^{-12}\right]^{a}$ (abs.)	3.74 ± 0.06	–	–
$N_{\rm H} = 0.71 \times 10^{22}$ cm^{-2}	$F\left[\times 10^{-12}\right]^{b}$ (unabs.)	5.68 ± 0.08	–	–
	χ^2_ν (DoF)	1.04 (1101)	–	–
	Photon Index Γ	$2.0^{+0.4}_{-0.5}$	–	–
e3-ring	kT (keV)	0.2 ± 0.1	–	–
$N_{\rm H} = 0.79 \times 10^{22}$ cm^{-2}	χ^2_ν (DoF)	1.14 (797)	–	–

Table A2. XSPEC fits using `const*tbabs*power` with the `cFlux` model added to acquire flux values. Column densities frozen to their best fit value using the XMM-Newton data. For the 'e3-ring' region, the additional component shown corresponds to a thermal (`mekal` in XSPEC) model with solar abundances. Quoted uncertainties for 90% C.L.

[a] Absorbed flux in erg cm^{-2} s^{-1}.

[b] Unabsorbed flux in erg cm^{-2} s^{-1}.

[c] For the joint 0.5–30 keV flux, we list the combined 0.5–10 keV (XMM) and 10-30 keV (NuSTAR) fluxes with the model parameters frozen to their best values from the joint fit.

[d] The larger 'e2' region encompassing the 'lenticular' region (see Figure 2) shows evidence of soft thermal X-ray emission with $kT \lesssim 0.2$ keV, however with the thermal parameters poorly constrained.

Telescopes

XMM-Newton

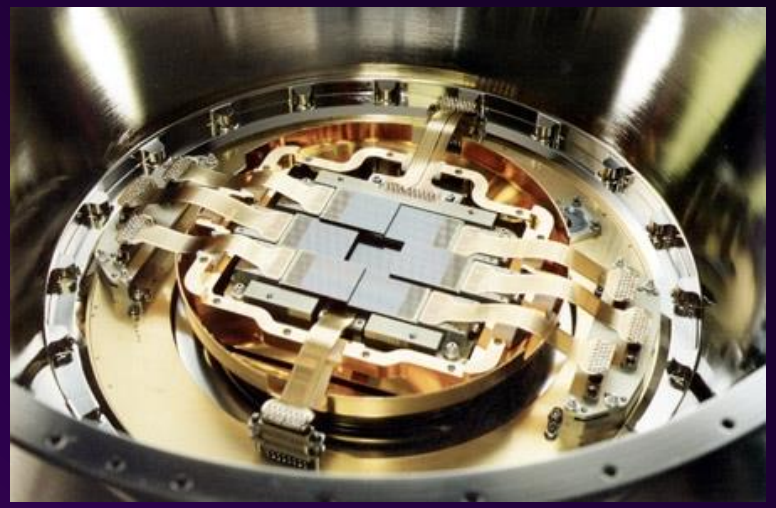

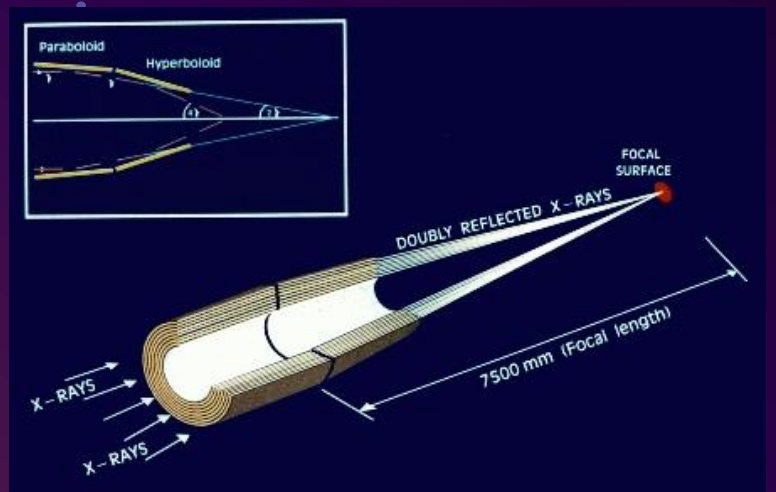

NuSTAR

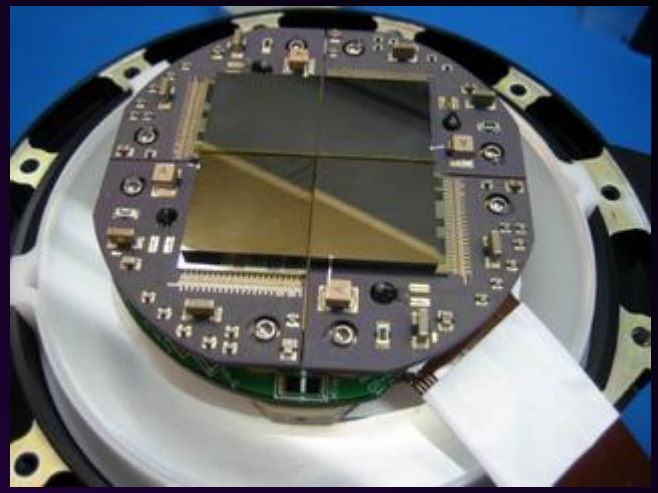

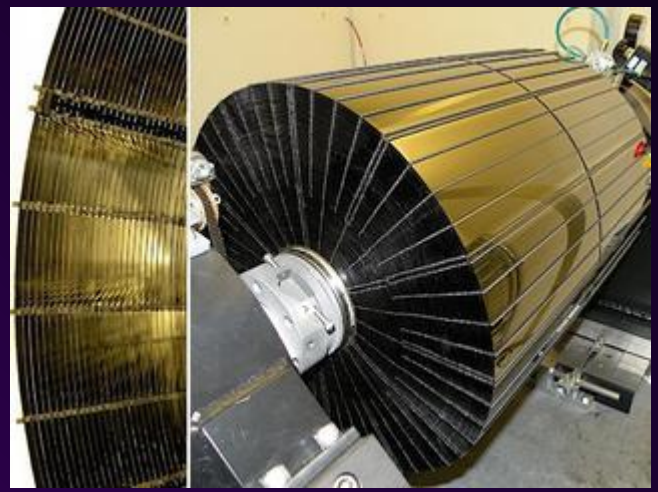

Chandra